GENERAL

Synchronization and Pattern Dynamics of Coupled Chaotic Maps on Complex Networks

To cite this article: Shen Yu *et al* 2008 *Chinese Phys. Lett.* **25** 3875

View the article online for updates and enhancements.

Related content

Recent citations

Synchronization and Pattern Dynamics of Coupled Chaotic Maps on Complex Networks

SHEN Yu(沈瑜), HOU Zhong-Huai(侯中怀)**, XIN Hou-Wen(辛厚文)

Hefei National Lab for Physical Sciences at Microscale, Department of Chemical Physics, University of Science and Technology of China, Hefei 230026

The synchronization and pattern dynamics of coupled logistic maps on a certain type of complex network, constructed by adding random shortcuts to a regular ring, is investigated. For parameters where an isolated map is fully chaotic, the defect turbulence, which is dominant in the regular network, can be tamed into ordered periodic patterns or synchronized chaotic states when random shortcuts are added, and the patterns formed on the complex network can be grouped into two or three branches depending on the coupling strength.

The dynamics of complex networks have gained great research interest in recent years.[1] Of most interest are the small-world (SW) networks proposed by Watts and Strogatz,[2] and the scale-free (SF) networks put forward by Barabási and Albert.[3] The SW network is characterized by a short average path length between the network nodes and a large clustering coefficient, and the SF one has a power-law degree distribution. It has been shown that network topology plays a crucial role in a system's dynamics, and a vast of literatures have been devoted to this topic. For instance, synchronization can be considerably improved on SW or SF networks,[4,5] any spreading rate can lead to whole infection of disease on SF networks,[6] the SF network shows high tolerance to error but not to attack,[7] SW neuron networks show fast response and enhanced coherent motion,[8] spatiotemporal chaos can be tamed by random shortcuts,[9] SW topology can eliminate oscillator death,[10] to list just a few.

In the present work, we have studied the synchronization and pattern dynamics of coupled logistic maps on a type of complex network, constructed by randomly adding shortcuts to a regular ring. Although the dynamics of chaotic maps on complex networks have already been investigated by many others, most results reported only accounted for spatial synchronization,[11−15] and it was shown that coupling topology and delay strongly influence the synchronization ability. Here we find that coupling topology also strongly influences the pattern dynamics. We set the parameter such that each isolated map is in fully developed chaos and defect turbulence is the dominant pattern in the regular network. We show that the defect turbulence can be tamed when random links are added, and the patterns formed on the SW-like network can be grouped into two or three branches, depending on whether the system is synchronizable or not.

We consider a coupled map lattice of the form

$$x_{n+1}(i) = f(x_n(i)) + \frac{\varepsilon}{K_i} \sum_{j \in \Omega(i)} \big[f(x_n(j)) - f(x_n(i)) \big], \quad (i = 1, \dots N), \qquad (1)$$

where $f(x) = \rho x(1 - x)$ stands for the logistic-map which is often cited as an archetypal example of how complex, chaotic behaviour can arise from very simple non-linear dynamical equations. Here $\varepsilon \in (0, 1)$ is the coupling strength, the summation of j runs over the neighbours of node i (denoted by $\Omega(i)$), K_i is the degree of node i, and $N = 256$ is the number of nodes. We choose the control parameter as $\rho = 3.825$, which is at the edge of the chaotic zone of a single map. The complex networks are constructed by adding M random links to a regular ring with periodic boundary condition (the largest allowed value of M is $N(N − 3)/2$). When M is not too large, the resulting network has SW feature as proposed by Newman and Watts,[16] and the random added links play the roles as shortcuts.

The main motivation of the present paper is to elucidate the interrelation between the network topology and the spatiotemporal dynamics of the system. We use the fraction of random links $q = M/[N(N − 3)/2]$ to characterize the network's topology, and q is changed from 0 to 1 in the simulation runs. For each value of q, random initial condition is chosen and the simulation is repeated after enough long transient time. In contrast to most previous studies that mainly focused on spatial synchronization, we also take into account the temporal regularity of the patterns. As usual, we introduce the standard deviation σ to measure the de-synchronization:

$$\sigma = \left\langle \sqrt{\left[\sum_{i=1}^N \frac{x_i^2}{N} - \left(\sum_{i=1}^N \frac{x_i}{N} \right)^2 \right] / (N-1)} \right\rangle, \quad (2)$$

where the brackets mean the averaging over time. Obviously, a smaller σ means more synchronization, and $\sigma = 0$ when the system is completely synchronized. As to the temporal regularity, we use the characteristic correlation time τ_c defined as[16]

$$\tau_c = \frac{1}{N} \sum_{n=1}^{N} \frac{1}{T} \int_0^T c_n^2(\tau) d\tau, \tag{3}$$

where $c_n(\tau) = \sum_{i=1}^{T} x_n(i) x_n(i+\tau)/x_n^2(i)$ is the normalized autocorrelation function of $x_n(i)$ with lag τ; T is the time interval to calculate $c_n(\tau)$ which can be chosen somewhat arbitrarily if being long enough. Apparently, a pattern periodic in time will have much larger τ than a chaotic one. Note that even when the pattern is not synchronized in space, τ_c could also be large because $c_n(\tau)$ is calculated before averaging over different sites n. Combining the information from σ and τ_c, one may obtain more qualitative information about the patterns.

In our simulation, we find that the final patterns observed depend strongly on whether the system can be synchronized or not. Therefore, we will firstly consider the synchronization problem. Actually, the synchronization of coupled chaotic oscillators, either described by continuous differential equations or by discrete maps, has been extensively investigated in the literature, and it is now generally accepted that the eigenvalues of the Laplacian matrix $\boldsymbol{A}$ of the network play a key role, rather than the coupling strength alone. For example, the local stability of the full-synchronized state is decided by the well-known 'master stability function', which characterizes how the Lyapunov exponents of the synchronized manifold depend on the coupling strength and the spectrum of the Laplacian matrix.[4] By definition, $A_{ij} = -K_i$, $(i = 1, 2, \ldots, N)$ are the negative degrees of node i, $A_{ii} = 1$ if node i and j are connected, and 0 otherwise.

For the system (1) considered in the present work, the necessary condition for the local linear stability of the synchronized state (SS) reads[14]

$$\frac{1 - e^{-\mu_0}}{\lambda_1} < \varepsilon < \frac{1 + e^{-\mu_0}}{\lambda_K}, \tag{4}$$

where μ_0 is the Lyapunov exponent of the map function f (for $\rho = 3.825$ in the present work, $\mu_0 \approx 0.41$); λ_1 and λ_K are the smallest and largest nonzero eigenvalues of the matrix $\boldsymbol{L}$ defined as $L_{ij} = \frac{1}{K_i} A_{ij}$, where A_{ij} are the elements of the Laplacian matrix $\boldsymbol{A}$. With the increment of q from 0 to 1, λ_1 increases monotonically from 0 to 1 and λ_K decreases monotonically from 2 to 1. By direct calculations we can check that if the first equality in Eq. (4) holds, so does the second one. Therefore, Eq. (4) defines a boundary line, $\varepsilon\lambda_1 = 1 - e^{-\mu_0}$, in the $\varepsilon \sim \lambda_1$ plane (as also in the

$\varepsilon \sim q$ plane), below which no SS occurs. The validity of this condition is shown in Fig. 1, where numerical results (open circles with error-bars) agree well with the theoretical predictions (the solid line).

One should note that the above discussions only address the local stability of the SS. This is the necessary condition for synchronization, but not a sufficient one, which requires that the system will definitely achieve the SS no matter what the initial condition is. By direct numerical simulations, we have also obtained the boundary of global stability in the $\varepsilon - q$ plane as indicated by the line with squares in Fig. 1. Therefore, we can divide the $\varepsilon - q$ parameter plane into three regions, as shown in Fig. 1. SS surely occurs above the upper line (squares), and it cannot happen below the lower line. A transient region lies between them, where the final state depends on the initial condition.
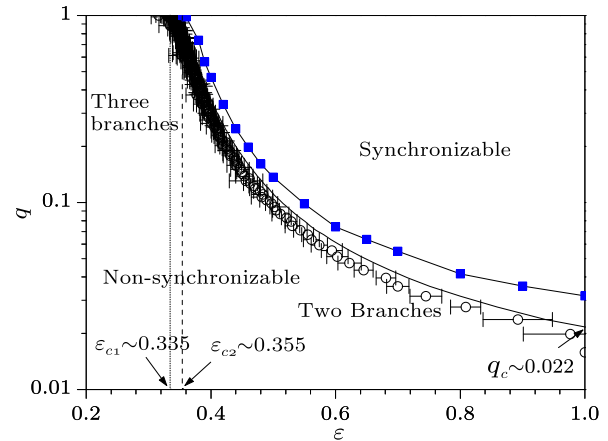

Fig. 1. Synchronization boundary for the coupled logistic-map lattice (see the context for details). For $\varepsilon < \varepsilon_{c1}$ or $q < q_c$, no synchronization can be attained. The dashed line separates the region with three branches to two branches in the non-synchronizable region. Here $\rho = 3.825$.

We now turn to the question how the system's dynamics evolves when the network topology changes with q from 0 to 1. Clearly, the coupling strength plays an important role. According to Fig. 1, for $\varepsilon > \varepsilon_{c2}$, the system will fall into the SS if q exceeds some critical value q_c, while for $\varepsilon < \varepsilon_{c1}$, no SS can be achieved even if the network is globally coupled. We find that whether the system can be synchronized or not plays a crucial role in the observed branching behaviour as described in the following.

In the synchronizable case ($\varepsilon > \varepsilon_{c2}$), the only stable state for $q > q_c$ is the SS, for which σ is 0 and τ_c is very small. However, for $q < q_c$, the patterns observed clearly branch into two types, for one the order parameters σ and τ_c both become larger (upper branch), and for the other they both decrease (lower branch). The upper branch terminates at a certain value of q, and the remaining lower branch changes continuously to

the SS. An example of such branching behaviour for $\varepsilon = 0.9$, which is larger than ε_{c2}, is shown in Fig. 2. We depict the scattering distribution of τ_c and σ for 100 simulation runs. Clearly, both quantities show two distinct branches. The upper branch has large τ_c and σ, i.e., the pattern is rather regular in time but not in space; while the lower branch has much smaller τ_c and σ, which becomes more and more chaotic in time and synchronized in space until finally it reaches the SS when q goes across q_c. Note that the higher branch disappears for $q \approx 0.013$ that is still away from $q_c \approx 0.027$. Typical patterns observed in this case are shown in Fig. 3. Figure 3(a) gives the defect turbulence observed in a regular network ($q = 0$). Figure 3(b) shows the SS for large q. Figure 3(c) presents the pattern of the higher branch with large τ_c and σ. Figure 3(d) is of the lower branch. In Fig. 3(c), each site in the lattice is already periodic in time, but the period is different for different nodes.
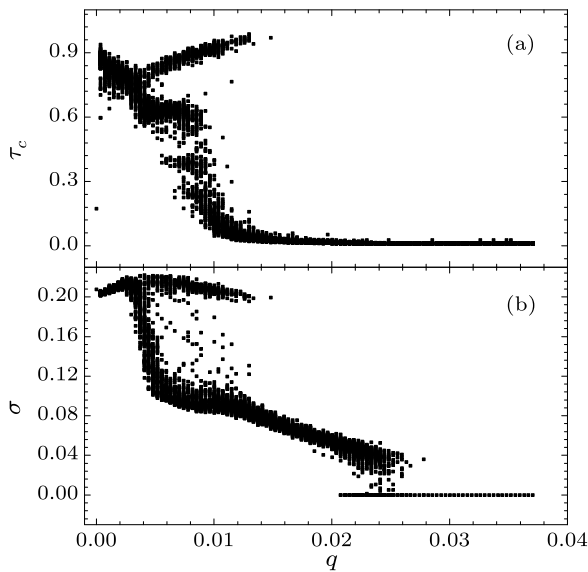
only allowed one for a globally coupled lattice ($q = 1$), while the other two disappear in the vicinity of $q = 1$. Typical patterns for $\varepsilon = 0.3$ is shown in Fig. 5. Figure 5(a) is the defect turbulence for $q = 0, 5$, Fig. 5(b) is the nearly periodic and synchronized pattern of the middle branch, Fig. 5(c) is the periodic but not synchronized pattern of the upper branch, and Fig. 5(d) is the disordered pattern of the lower branch.
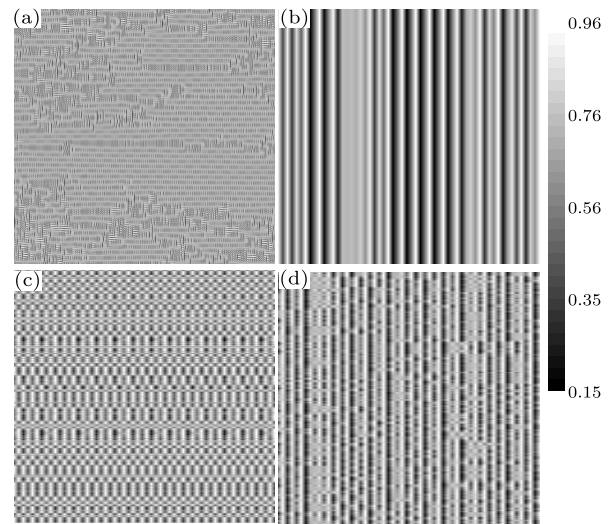

Fig. 3. Typical patterns observed for $\varepsilon = 0.9$. (a) Defect turbulence in the regular lattice. (b) Synchronized chaotic state for $q = 0.037$. (c) The higher branch: $q = 0.0111$, $\tau_c = 0.9429$, $\sigma = 0.2028$. (d) The lower branch: $q = 0.0111$, $\tau_c = 0.0437$, $\sigma = 0.0897$. Note: the time scale in (a) is 10 times larger than the others.
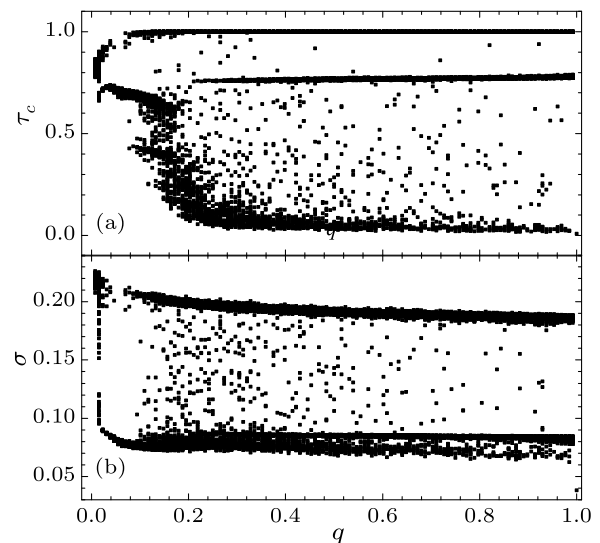

Fig. 2. Dependence of (a) distribution of τ_c, (b) distribution of σ on q. The coupling strength is $\varepsilon = 0.9$.

For $\varepsilon < \varepsilon_{c1}$, no synchronization can occur even when $q = 1$. In this case, three branches are observed, indicating some kind of multi-stability of the system's dynamics (Fig. 4). The upper branch has large τ_c and σ, which resembles the high branch for $\varepsilon = 0.9$. When exceeds some value, this branch of pattern becomes exactly periodic in time, for which τ_c is exactly 1. The lower branch has small τ_c and σ, which also looks like the lower branch for $\varepsilon = 0.9$, but no synchronization in space can be attained when q increases. Of more interest is the middle branch that appears for the case that q exceeds a certain value, not observed in the strong-coupling case. This branch of pattern has rather large τ_c (about 0.8) and small σ, indicating that it is nearly periodic in time and synchronized in space. It is also shown that the middle branch is the

Fig. 4. Dependence of (a) distribution of τ_c, (b) distribution of σ on q. The coupling strength is $\varepsilon = 0.3$.

The findings of present work reveal some interesting roles of network topology on the pattern dynamics of coupled chaotic maps. Although only defect turbulence can be observed in the regular network (for the

parameter $\rho = 3.825$), more features are found when a certain fraction of random links are added. Depending on the coupling strength and number of additional links, one may observe ordered periodic patterns or synchronized chaotic patterns. Therefore, we demonstrate a further example that 'random shortcuts can tame spatiotemporal chaos', as already reported in our previous studies on coupled differential dynamical systems.[9,18]
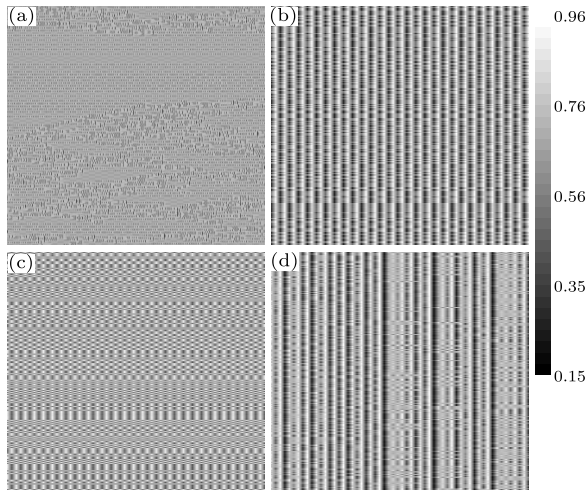

Fig. 5. Typical patterns observed for $\varepsilon = 0.3$: (a) defect turbulence in the regular lattice, (b) the middle branch: $\tau_c = 0.76$, $\sigma = 0.086$, (c) the high branch: $\tau_c = 1$, $\sigma = 0.19$, (d) the low branch: $\tau_c = 0.070$, $\sigma = 0.078$. For (b)–(d), $q = 0.32$. Note: The time scale in (a) is 10 times larger than the others.

According to Ref. [19], there are mainly six types of patterns for one-dimensional coupled logistic lattice, i.e., frozen random pattern, pattern selection, defect chaotic diffusion, defect turbulence, pattern competition intermittency, and fully developed turbulence, depending on the parameter values of ε and ρ. All the six patterns have their attractive basins, the boundaries between which are not that sharp. According to this picture, Figs. 3(c) and 5(c) can be classified into a pattern selection, Figs. 3(d) and 5(d) belong to fully developed turbulence, and Figs. 3(a) and 5(a) are defect turbulence. Hence, it seems that topological disorder has induced somewhat transition from defect turbulence to fully developed turbulence or pattern

selection. In addition, Figs. 3(b) and 5(b) are not observed in regular network, indicating that new types of pattern can be formed on complex networks.

In summary, we have studied the pattern dynamics of coupled logistic-maps on small-world like networks, constructed by adding random links to a regular ring. The parameter is chosen such that spatiotemporal chaos is observed in the original regular network. We define the characteristic time τ_c and spatial deviation σ as a quantitative measure of the spatiotemporal order of the pattern. With the increasing number of random links, the distribution of τ_c and σ show two or three branches depending on the coupling strength, indication multi-stability of the dynamics and new types of patterns are formed by taming the chaos. It is our hope that the present work could open more perspective on the study of pattern dynamics on complex networks.

References

[1] Albert R and Barabási A L 2002 *Rev. Mod. Phys.* **74** 47
[2] Watts D J and Strogatz S H 1998 *Nature* **393** 440
[3] Barabási A L and Albert R 1999 *Science* **286** 509
[4] Barahona M and Pecora L M 2002 *Phys. Rev. Lett.* **89** 054101
[5] Motter A E, Zhou C S, and Kurths J 2005 *Phys. Rev.* E **71** 016116
[6] Eguíluz V M and Klemm K 2002 *Phys. Rev. Lett.* **89** 108701
[7] Albert R, Jeong H and Barabási A L 2000 *Nature* **406** 378
[8] Lago-fernández L F, Huerta R, Corbacho F, and Sigüenza J A 2000 *Phys. Rev. Lett.* **84** 2758
[9] Qi F, Hou Z H, and Xin H W 2003 *Phys. Rev. Lett.* **91** 064102
[10] Hou Z H and Xin H W 2003 *Phys. Rev.* E **68** 055102
[11] Atay F M and Jost J, Wende A 2004 *Phys. Rev. Lett.* **92** 144101
[12] Masoller C and Martí A C 2005 *Phys. Rev. Lett.* **94** 134102
[13] Gade P M and Hu C K 2000 *Phys. Rev.* E **62** 6409
[14] Jost J and Joy M P 2001 *Phys. Rev.* E **65** 016201
[15] Lind P G, Gallas J A C and Herrmann H J 2004 *Phy. Rev.* E **70** 056207
[16] Newman M E J, Moore C and Watts D J 2000 *Phys. Rev. Lett.* **84** 3201
[17] Pecora L M and Carroll T L 1998 *Phys. Rev. Lett.* **80** 2109
[18] Wang M S, Hou Z H and Xin H W 2006 *Chem. Phys. Chem.* **7** 579
[19] Kaneko K 1989 *Physica* D **34** 1